Multioffset 3-C VSP processing and coal-seam anisotropy: An Alberta case history

Zandong Sun, Peter Manning* and R. James Brown

ABSTRACT

Alberta coal causes imaging ambiguities in the case of a reef underneath coal on conventional seismic data in areas where coal is present. A multioffset 3–C VSP experiment was carried out in a 3–D prospect area. The data were processed for a comparison of resolution between 3–D surface data and multioffset VSP and as a coal anisotropy study. Converted-wave processing is employed in this paper, and the anisotropic feature due to coal fracture is presented. The time shift (about 6 ms) between the radial- and transverse-component CCP stack sections is due to a group of dominant fractures oriented SE–NW. It is much easier for shear waves to propagate through a coal medium than compressional waves.

INTRODUCTION

Shear-wave seismic data are more and more widely used in hydrocarbon exploration. They provide significant information that can not be extracted from compressional-wave data. It is probably the most direct and sensitive type of data available for deducing rock-fracture properties from remote measurement (Winterstein, 1992). Through shear-wave splitting analysis, one can identify and characterize the vertical fracture system (Crampin, 1985). If shear waves contained the same frequencies as compressional waves, they would provide much greater resolution of geological information because of the lower velocity of the shear waves. However, the surface shear-wave data rarely show any increase in resolution compared to *P*-wave data due to greater absorption in the weathering layer. VSP converted-wave data have better quality because of the method of data acquisition. In this experiment four vibroseis sources (frequency 8-84 Hz) denoted *A*, *B*, *C*, *D* were used simultaneously. The polarities of sweeps for the different sources were varied.

One single three-component geophone was moved up from 1460 m to 700 m at 10 m interval. At each location four different sweeps were applied simultaneously, for four different combinations of polarities (Table 1), giving four records for each component (R_1, R_2, R_3, R_4). After some algebraic operations, the four components of interest can be sorted out for each source.

$$\begin{aligned} A &= R_1 + R_2 + R_3 + R_4 \\ B &= (R_1 + R_2) - (R_3 + R_4) \\ C &= (R_1 - R_2) + (R_3 - R_4) \\ D &= (R_1 - R_2) - (R_3 - R_4). \end{aligned} \tag{1}$$

* Mobil Oil Canada

The survey geometry is shown in Figure 1.

Table 1. Sweeps and offset distances for four sources

source	sweep				offset (m)
	1	2	3	4	
A	+	+	+	+	736.34
B	+	+	–	–	793.92
C	+	–	+	–	813.22
D	+	–	–	+	821.30

Table 1. Sweeps and offset distance for four sources

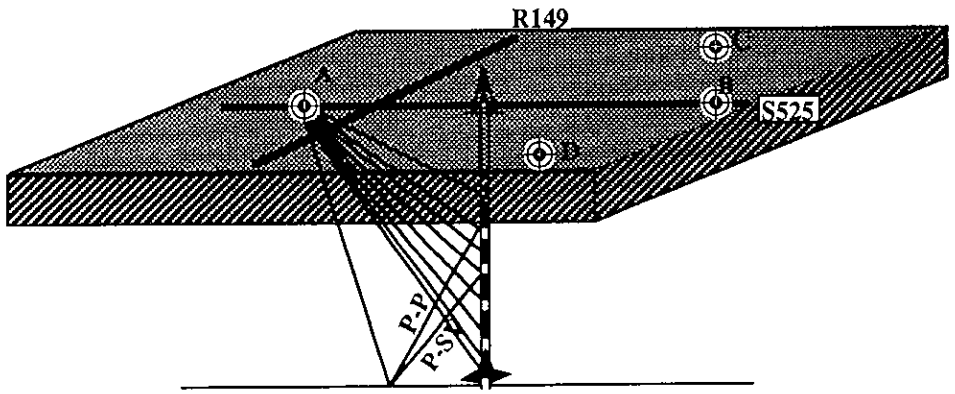

Figure 1. Multioffset VSP survey geometry.

3–C multioffset VSP can provide us three-dimensional information, so the data could be used for reef imaging, multidirectional crack studies, etc. Alberta coal seams which are widely distributed give rise to one of the tougher problems in hydrocarbon exploration. These coal seams often cover Devonian reservoir rock. They absorbs most of the incident seismic-wave energy, making it more difficult to image Devonian reefs. This study examines coal-seam anisotropy by employing converted-wave data through 3-C VSP processing.

PROCESSING

Converted-wave data processing is carried out with a view to studying anisotropy. Shear-wave anisotropy in the earth causes shear-wave splitting. Shear wave processing includes both radial and transverse components. However, to date, most three-component downhole phones do not have systems to measure downhole orientation. As the geophone is moved up, it rotates and randomly orients two horizontal components. So the effective removal of random orientation of two horizontal components must be done before any further processing. Rotation of horizontal components has been carried out by employing mathematical principles derived by DiSiena et al.(1984):

$$tan2\theta = \frac{2\,X\,Y}{XX - YY} \tag{2}$$

where XY is the zero-lag crosscorrelation between the two horizontal channels, and XX and YY are the zero-lag autocorrelations of each of the horizontal channels.

In practice, the downgoing P-wave (first break), which is the most obvious and consistent reference event in a VSP trace, was used to determine the time window. The correlations were calculated inside this window centered on the first P-wave breaks. The crosscorrelation between P-wave and rotated maximized horizontal component (radial component) was used to determine polarity of the radial component. As expected, the first downgoing P-wave break has been maximized on the radial component and minimized on the transverse component. The consistent angle between all sources, measured from surface and calculated from rotation, match well to each other.

Minimum-phase and dephasing deconvolution were applied to these vibroseis data. They gave a significant improvement of signal-to-noise ratio especially for the two horizontal components. The removal of the downgoing wavefield and the P-S mode separation were done by applying the p-t decomposition algorithm developed by Cheadle (1988). 5-trace and 7-trace local windows were used respectively for the p-t decompositions. A 5-trace window was found to be more suitable for the data. Tube waves were removed also by p-t decomposition utilizing the event slope difference relative to that of an upcoming shear wave. The velocity function was set up in a complicated way due to sonic-log measurement failure in the cased part of the well. Basically, P-wave velocities in the depth range of 400 to 1130 m/s are from near-offset VSP velocity analysis, S-wave velocities are based on a V_P/V_S ratio of 1.8. Both P-and S-wave logs are valid in the interval from 1130 to 1460 m. A P-wave sonic log in an adjacent well was used for the interval of 200 m-400 m and the assumption of a V_P/V_S ratio of 2.0 was made. The shear-wave mapping was performed by applying the equation developed by Stewart (1988,1989).The reflector offset distance is defined by:

$$X_r = \frac{X}{1 + \dfrac{\tilde{V}_{PN}^2\, T_{PN}}{\tilde{V}_{SNM}^2\, T_{SNM}}} \tag{3}$$

where V_{PN}, T_{PN} are downgoing P-wave RMS velocity, and V_{SNM} and T_{SNM} are upcoming S-wave RMS velocity and zero-offset traveltime, respectively. X and X_r are source-offset distance and reflectorpoint offset distance. The reflected converted wave traveltime from source to receivers is given by:

$$t = T_{PN} + T_{SNM} + \frac{X}{2\,(\tilde{V}_{PN}^2 T_{PN} + \tilde{V}_{SNM}^2 T_{SNM})} \tag{4}$$

The program coded according to these equations does NMO correction (two-way normal incidence P-wave time) and CCP binning in the same step trace by trace. After NMO and binning are applied to all input trances, a CCP map can be obtained according to bin size specified in the input deck. The CCP maps for source A and for the two horizontal components are depicted in Figure 2 (radial component) and Figure 3 (transverse component). As expected, the top reflectors are quite flat. The reflectors become slightly dipping in the coal unit (around 0.9 s) and dip quite considerably in the reef unit. The VSP converted-wave processing flow is listed in Table 2.

Table 2. Processing sequence and parameters for *VSP* horizontal channels data

DEMULTIPLEX.
ROTATION OF HORIZONTAL COMPONENTS
TRACE EQUALIZATION
SPIKING DECONVOLUTION
(Minimum phase and dephasing)
80-ms operator, 0.1% prewhitening
P-S MODE SEPARATION (5-trace local window).
MUTE
BANDPASS FILTER (8-40 Hz)
NMO, BINNING and CCP STACK
BANDPASS FILTER (8-40)
F-K FILTER

BIREFRINGENCE ANALYSIS FOR ALBERTA COAL VSP *P-SV* DATA AND THE SIGNIFICANCE TO CONVENTIONAL DATA.

Multioffset VSP data analysis

As mentioned above, a significant amount of seismic energy is attenuated after it propagates through a coal unit, and it creates considerable ambiguity in interpreting the reservoir unit below the coal. It is thus hard to image Devonian reefs because most of them are underneath the coal.

Shear-wave birefringence occurs only in anisotropic solids and is diagnostic of anisotropy. This can be related to rock properties and to the symmetry properties of the fractures. Significant energy has shown up on the minimized (transverse) component for both the A and B sources. after data rotation and deconvolution. It is not believed due to rotation error because there is a significant amount of time shift (about 10 ms On the first trace) (Figures 4a and 4b). This does not happen on data for sources C and D. The time shift between radial and transverse components on the CCP maps is about 6 ms for source$A$ (Figure 5) and about the same amount of time shift for source B. The

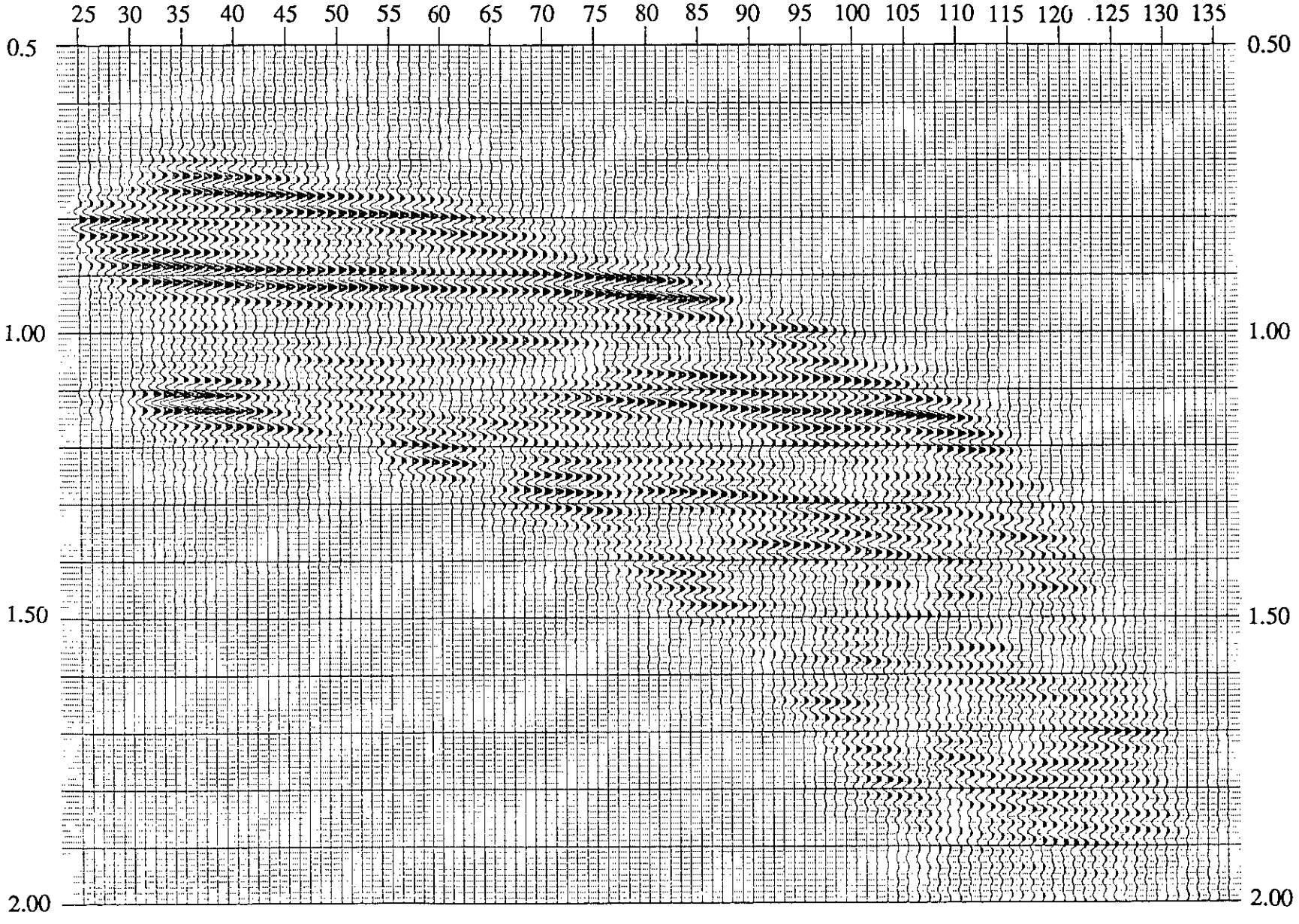

Figure 2. Converted wave radial component CCP map for A source, data plotted in P-wave time, trace interval 2.0 m.

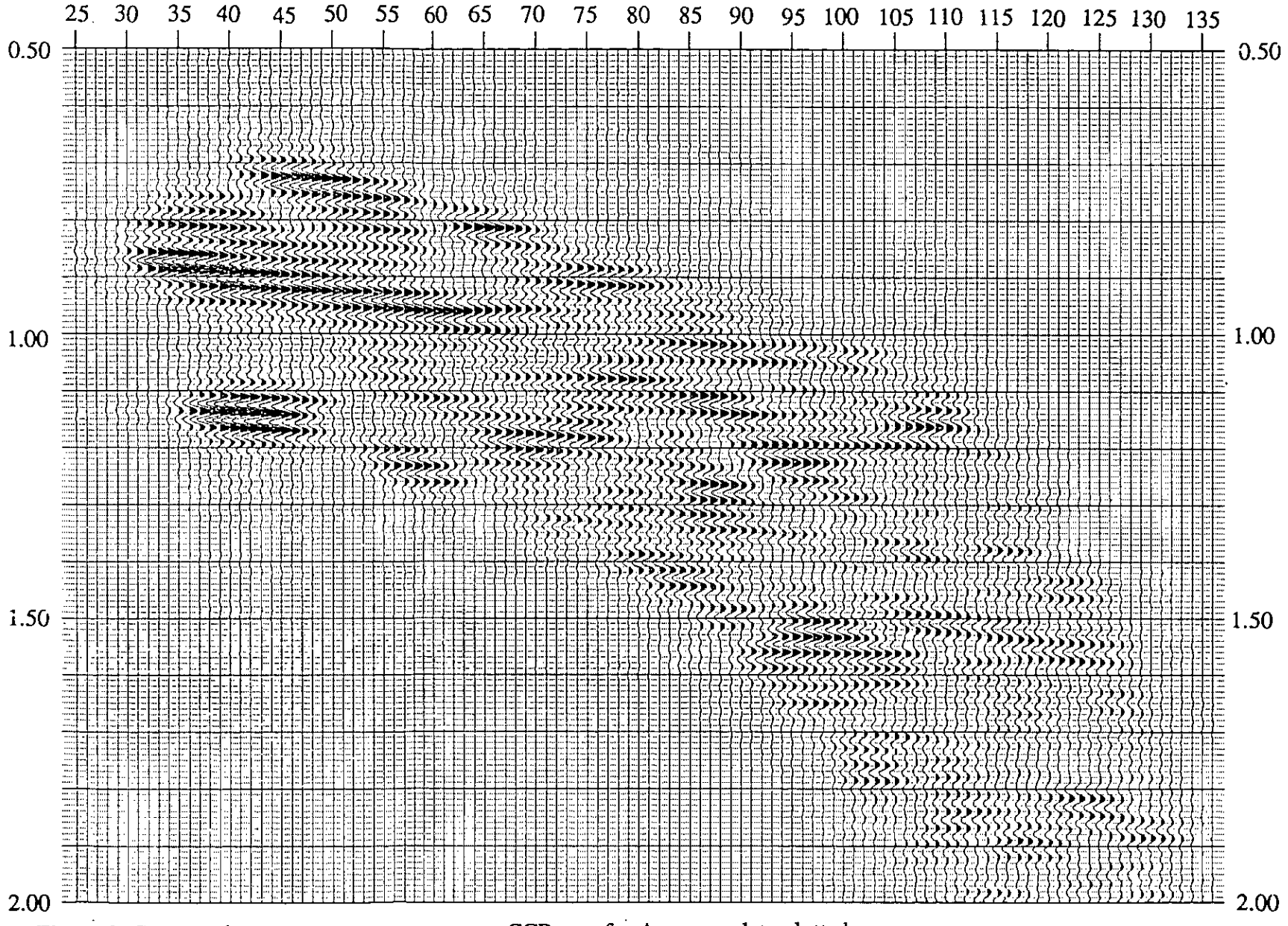

Figure 3. Converted wave transverse component CCP map for A source, data plotted in P-wave time, trace interval 2.0 m.

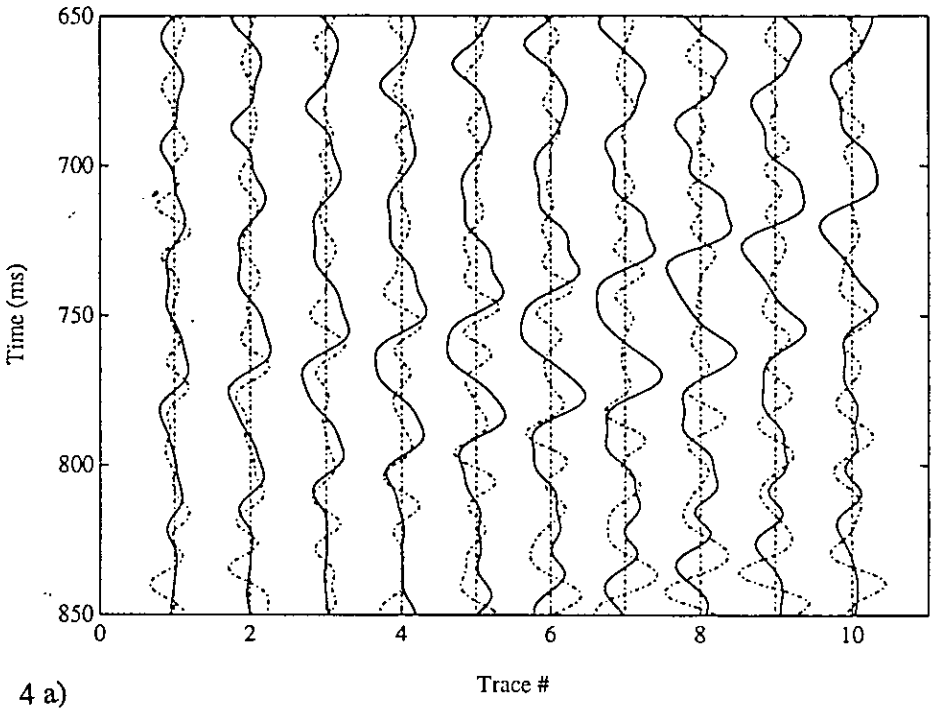

4 a)

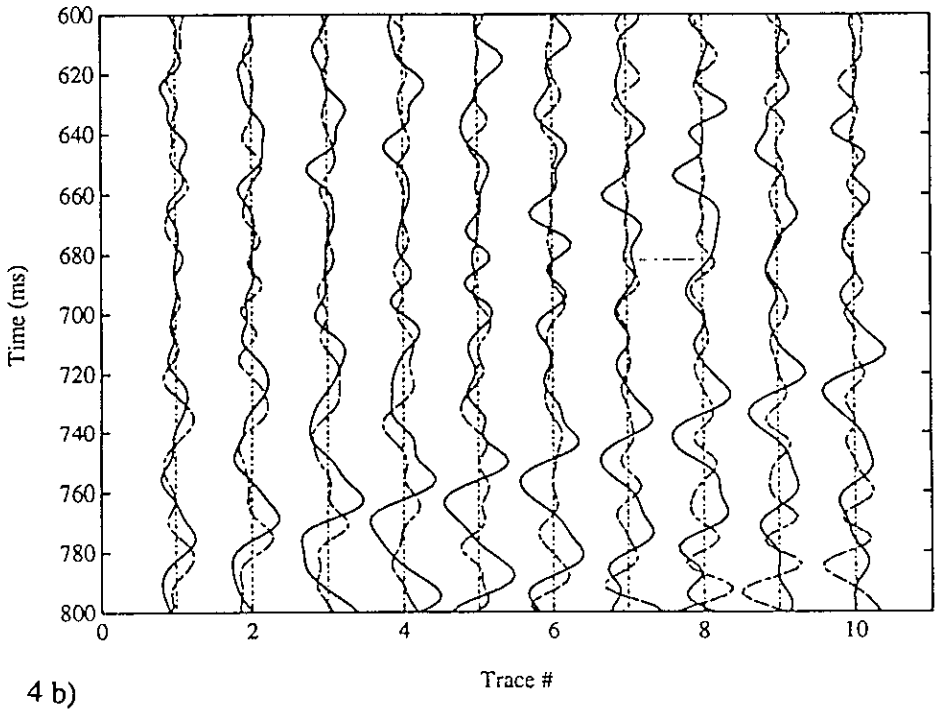

4 b)

Figure 4. Shear-wave birefringence illustrated with VSP upcoming converted wave data from A (4a) and B (4b) source. The Radial component (solid curves) arrives progressively earlier than the transverse component (dashed curves).

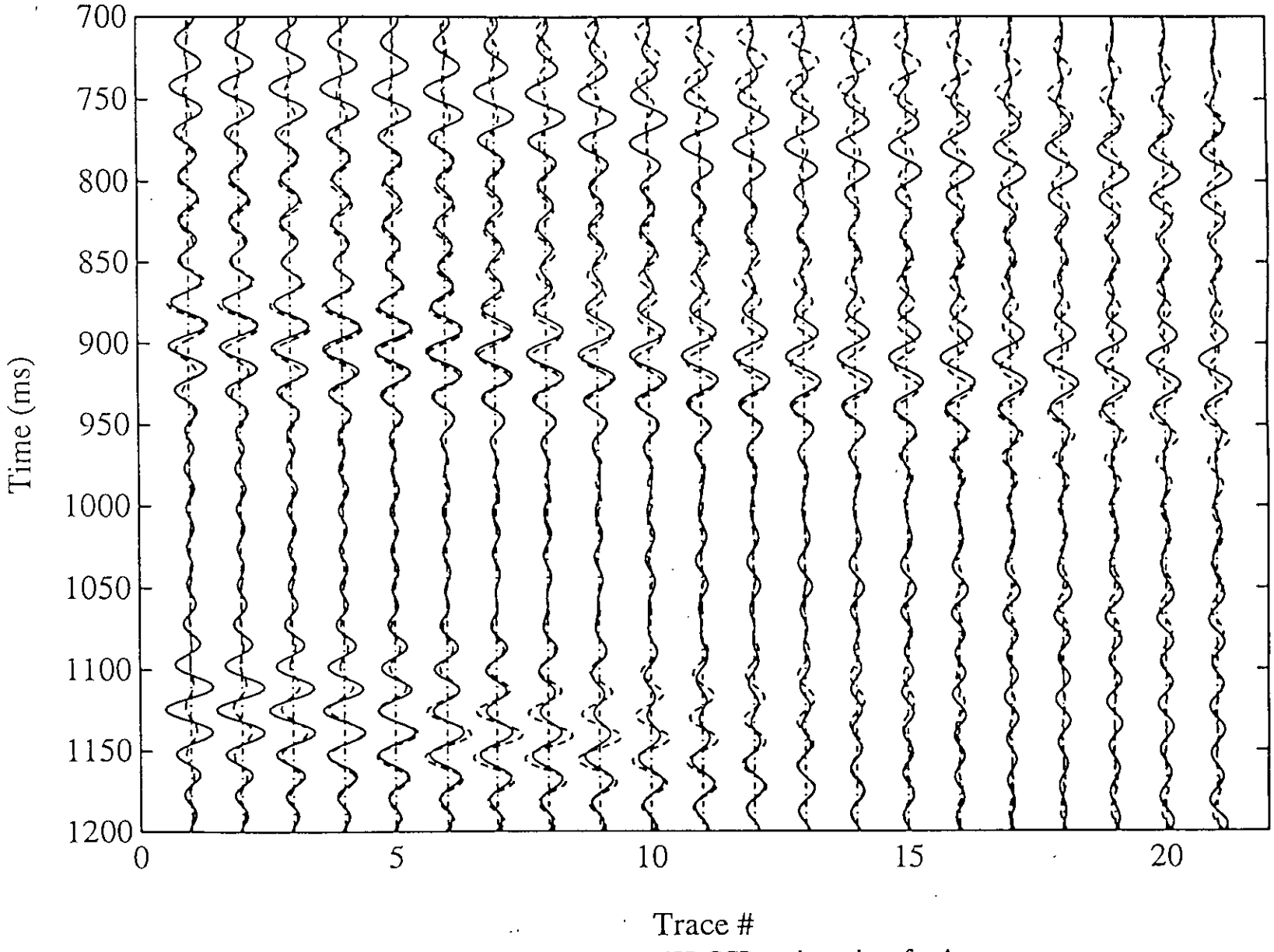

Figure 5. Shear wave birefringence illustrated with VSP CCP stack sections for A source. Radial component (sold curves) is earlier than transverse component (dashed curves).

birefringence analysis method presented here is embodied in an algorithm developed by Harrison (1992), called the θ–δ (rotation angle-time delay) analysis method. It relies on the modelling of crosscorrelations between rotated radial and transverse components, rather than the modelling of instantaneous polarization direction and amplitudes of the data themselves (Spencer and Chi, 1991). The processing sequence for birefringence analysis is slightly different. and the basic processing flow for birefringence analysis is listed in Table 3.

Table 3 VSP converted-wave processing sequence for birefringence analysis

DEMULTIPLEX
ROTATION OF HORIZONTAL COMPONENTS.
BANDPASS FILTER
P-S MODE SEPARATION
BANDPASS FILTER
NMO, BINNING AND STACK
BANDPASS FILTER.

The birefringence analysis is performed by sweeping through a two-dimensional set of natural-coordinate-system angle /time delay values for each θ–δ pair. This analysis was done over 80 traces on two components of each CCP stack section for all sources within the time window of 800–1100 ms. The contour-plotted result for source *A*, *B*, *C* and *D* are depicted in Figure 6a, b, c, and d respectively. It is indicated in Figure 6a that about 6 ms birefringence is present in the area on the line connecting source *A* to the well mouth, and the dominant fracture direction is 75° clockwise from the line. The result for the *B* source (Figure 6b) shows three groups of contours. It has a peak at $\theta = 82°$ and $\delta = 6$ ms shown on reliable contour which basically agrees with the result from source *A* on the identification of fracture orientation . The results for source *C* (Figure 6c) and *D* (Figure 6d) indicate that either no shear-wave splitting occurs in the area, or that the lines fall on principal axes. The geometry relationship on the surface is depicted in Figure 7. Assuming the fracture goes along the direction indicated by source *A* and *B*, and integrating all the information, we can probably conclude that there is a dominant single set of fractures (transversely isotropic rock with horizontal symmetry axis). The connecting lines between source and well mouth for *C* and *D* are close to principle axes. And this probably explains why shear-wave splitting is not seen on horizontal components of either source *C* or *D* . The results fit the regional fracture-orientation pattern.

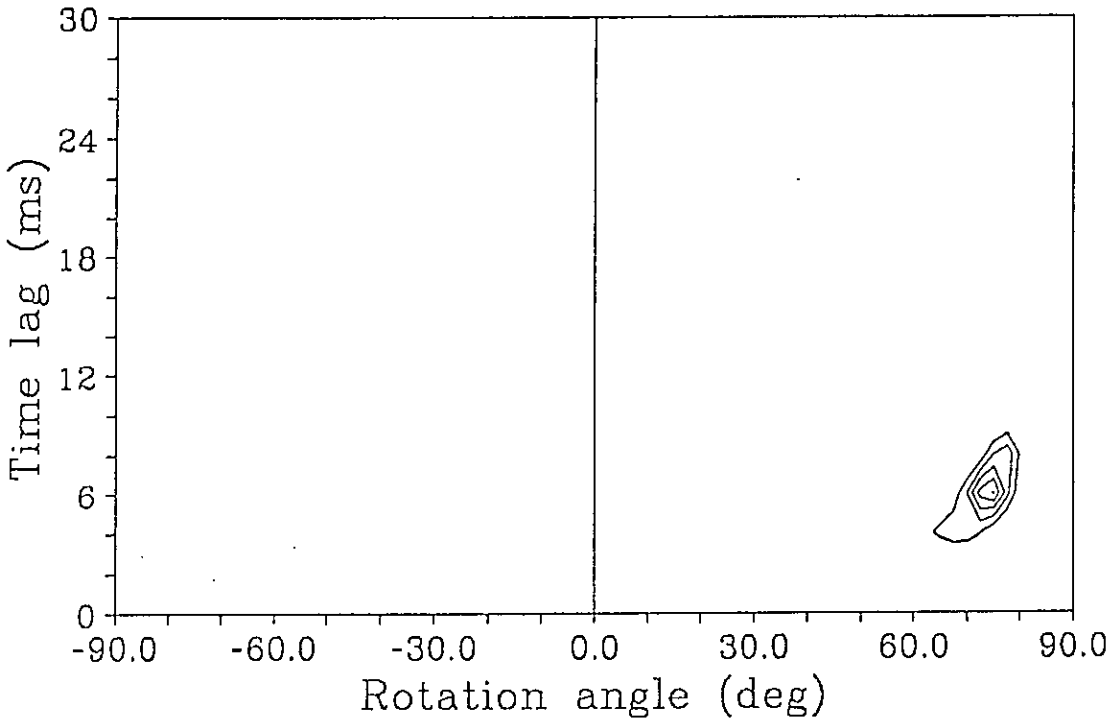
30
24
18
12
6
0
Time lag (ms)
-90.0
-60.0
-30.0
0.0
30.0
60.0
90.0
Rotation angle (deg)

6 a)

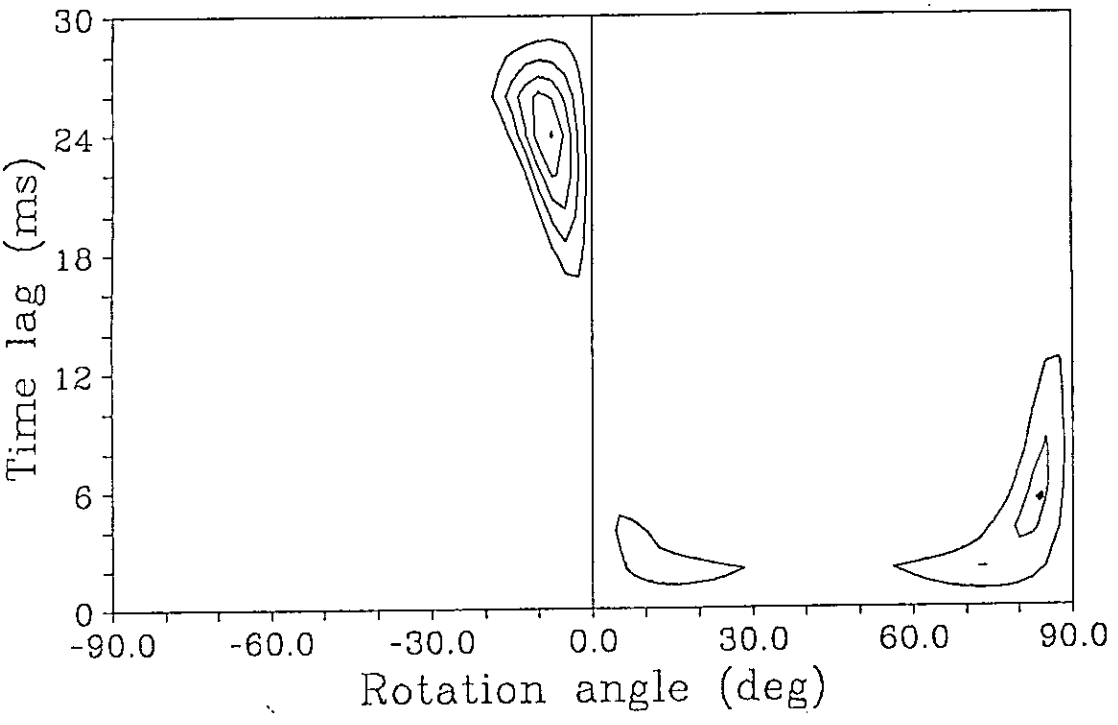
30
24
18
12
6
0
Time lag (ms)
-90.0
-60.0
-30.0
0.0
30.0
60.0
90.0
Rotation angle (deg)

6 b)

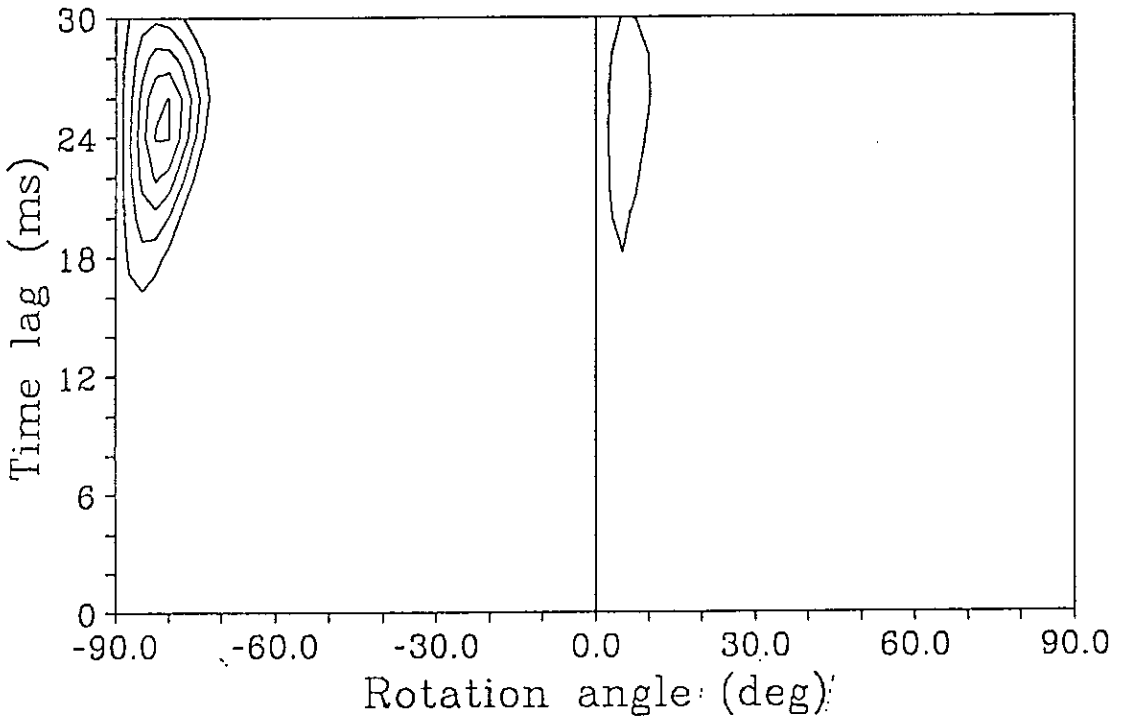

6 c)

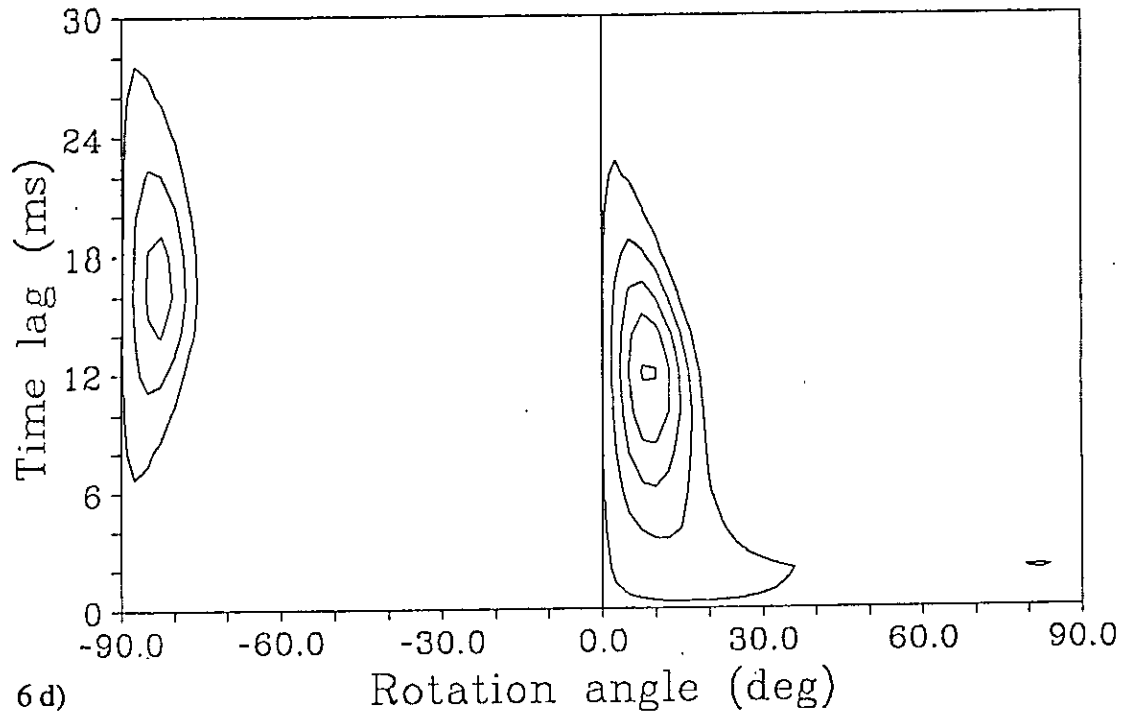

6 d)

Figure 6 Fracture orientation θ–δ analysis

(a) θ=75°, δ=6 ms for A source

(b) θ=82 , δ=6 ms for B source

(c) for C source

(d) for D source

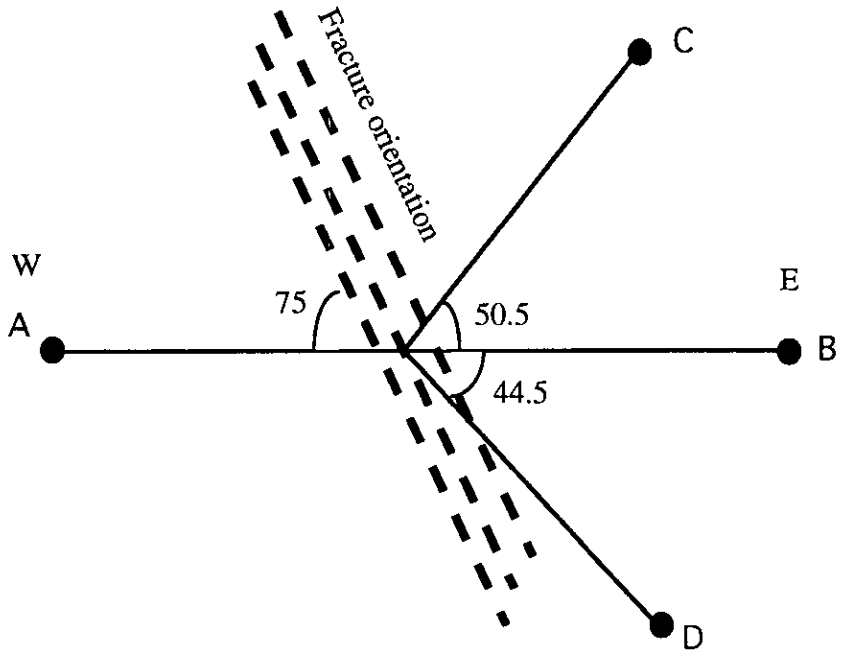

Figure 7. Plan view of dominant fractures and surface VSP source geometry

Physical modelling study

To add more understanding of the properties for both *P* and *S* waves as they propagate through the coal medium, we have set up the physical modelling experiment which is similar to that by Sun et al (1991) and tested one coal sample (10 cm in length, 8.8 cm in diameter). The frequency scaling was 10,000:1, and distance and time scaling 1:10,000. The source frequency for both *S* and *P* waves are the same, which is about 50 Hz (scaled). A coal sample was collected from Alberta area and the dominant fracture is depicted in Figure 8. Both P-and S-waves were recorded with different polarization in following three orientations:

long axis direction.

short axis direction, perpendicular to the dominant fracture.

short axis direction, parallel to the fracture.

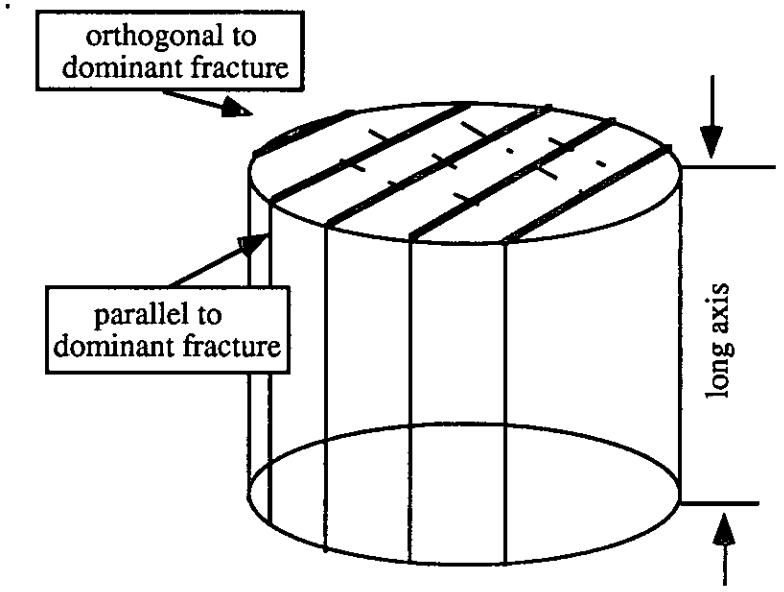

Figure 8. Sketch of fractured coal core used in modelling, bold lines represent dominant fractures.

The results produced an unexpected picture, and it results in a greater understanding of conventional seismic data. The shear wave has less attenuation than the *P* wave, and this is supported by records from all directions. It should be noted that both *P*-wave and *S*-wave sources have the same frequency content and the same amount of energy and that on the *P*-wave records there is nothing but noise (Figure 9 b and d). There is more absorption of P and S waves while they propagate in a vertical direction (long-axis direction in Figure 8; but shear-wave records show some energy propagation through this direction; see Figure 9 d) than in the horizontal direction. We presume that this has something to do with the geological process of coal deposition. Statistically, it is more layered in the vertical direction than the horizontal direction (Figure 9a and b). The direction of least attenuation is in the short-axis direction where waves propagate in the direction which is parallel to fractures. Shear waves show up quite nicely and signal/noise ratio is much higher than on other records (Figure 9c).

CONCLUSION

Although stress-induced shear-wave data sometimes can be very complicated, this study has shown multioffset VSP converted-wave data is probably the best for reservoir characterization and fracture study. The dominant fractures in the work area are oriented in the SE–NW direction. Shear–wave data (practically converted wave data) quality is probably much better than compressional wave data when propagating through the coal medium. Seismic attenuation in a coal layer varies with direction of wave propagation, being greater across fractures and less parallel to fractures. The horizontal direction in the fracture plane is the direction of least attenuation.

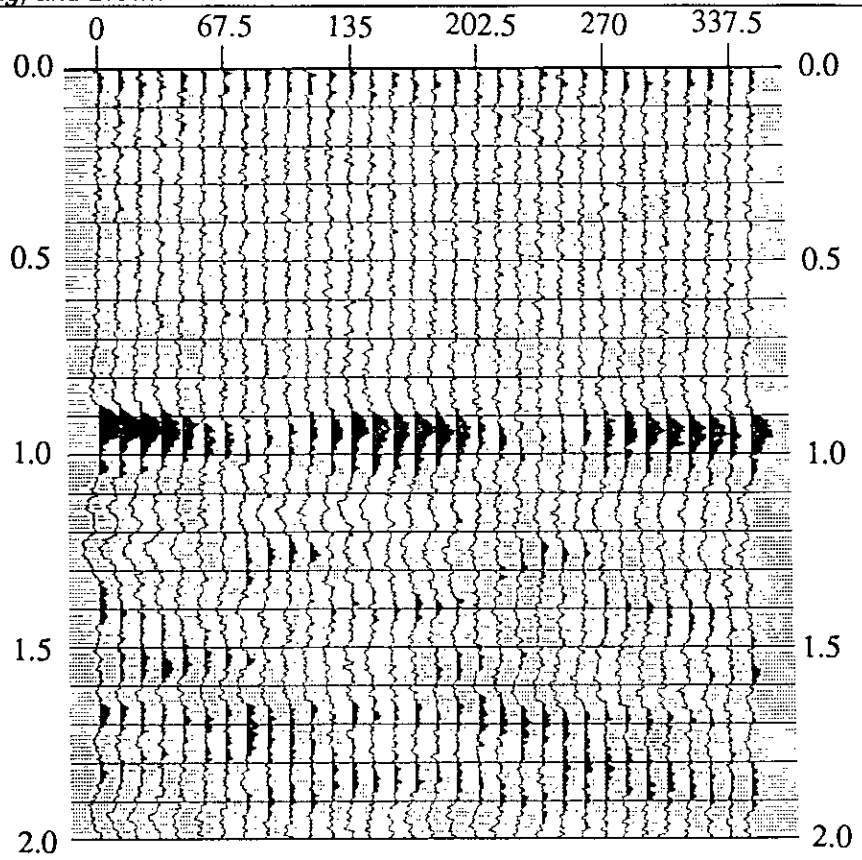
0
67.5
135
202.5
270
337.5
0.0
0.5
1.0
1.5
2.0

9 a)

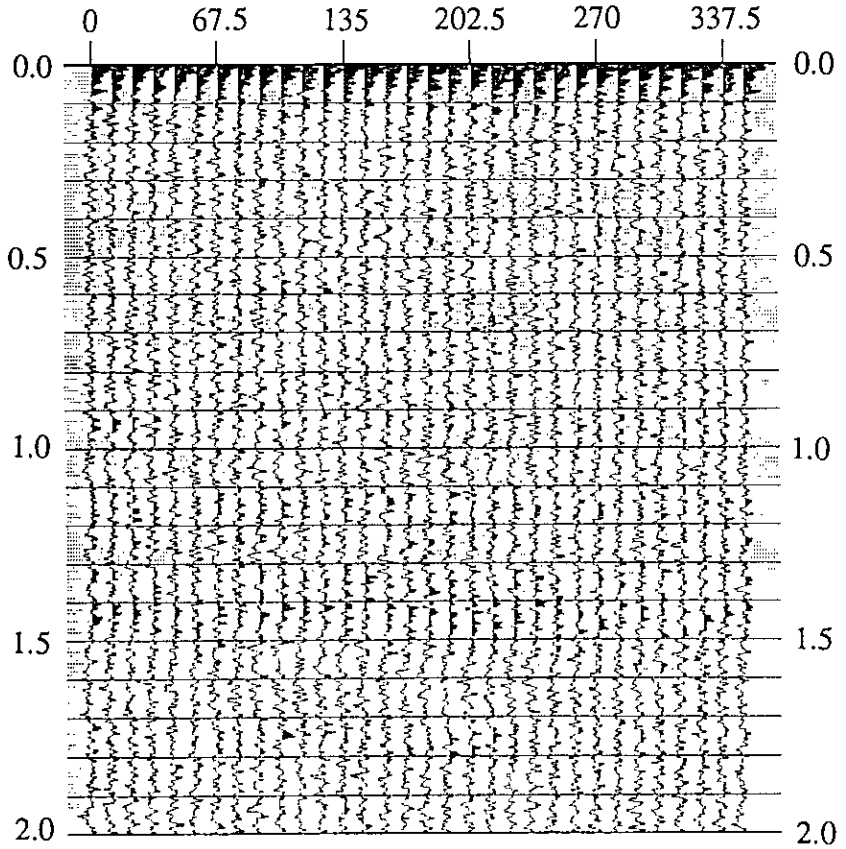
0
67.5
135
202.5
270
337.5
0.0
0.5
1.0
1.5
2.0

9 b)

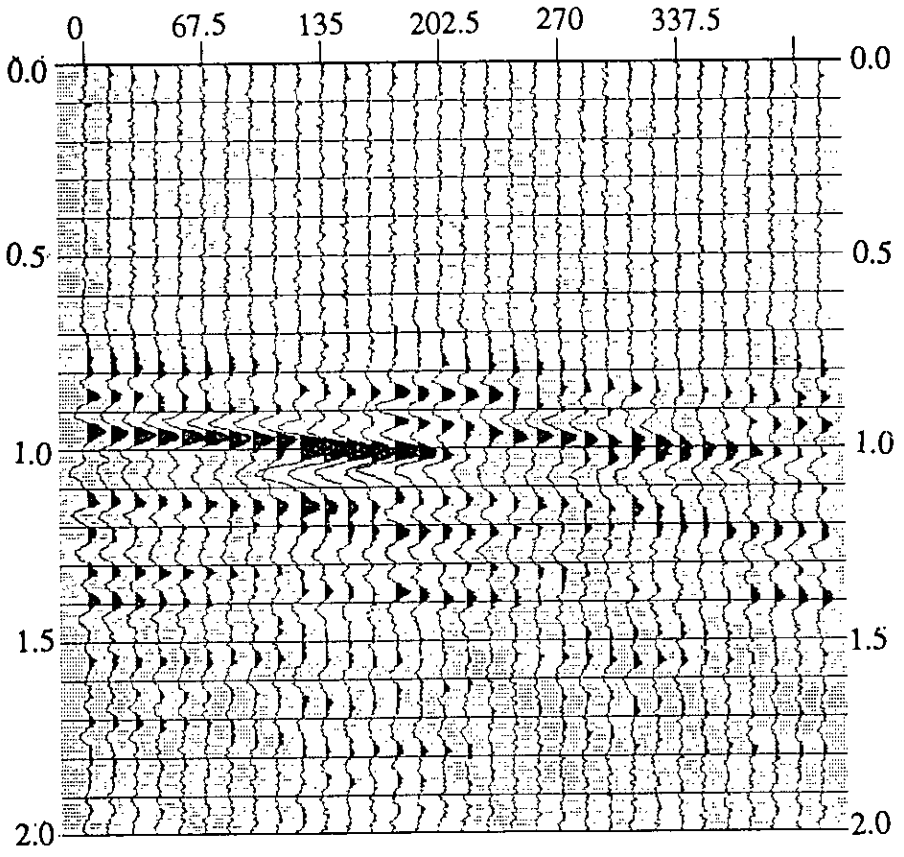
0
67.5
135
202.5
270
337.5
0.0
0.5
1.0
1.5
2.0

9 c)

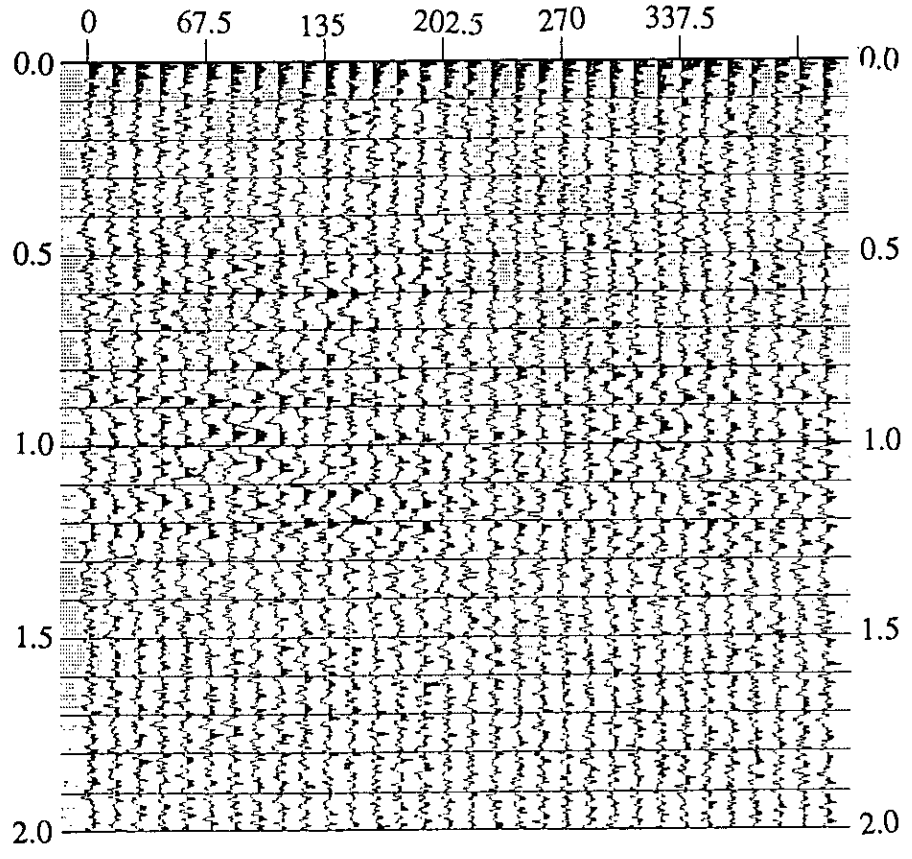
0
67.5
135
202.5
270
337.5
0.0
0.5
1.0
1.5
2.0

9 d)

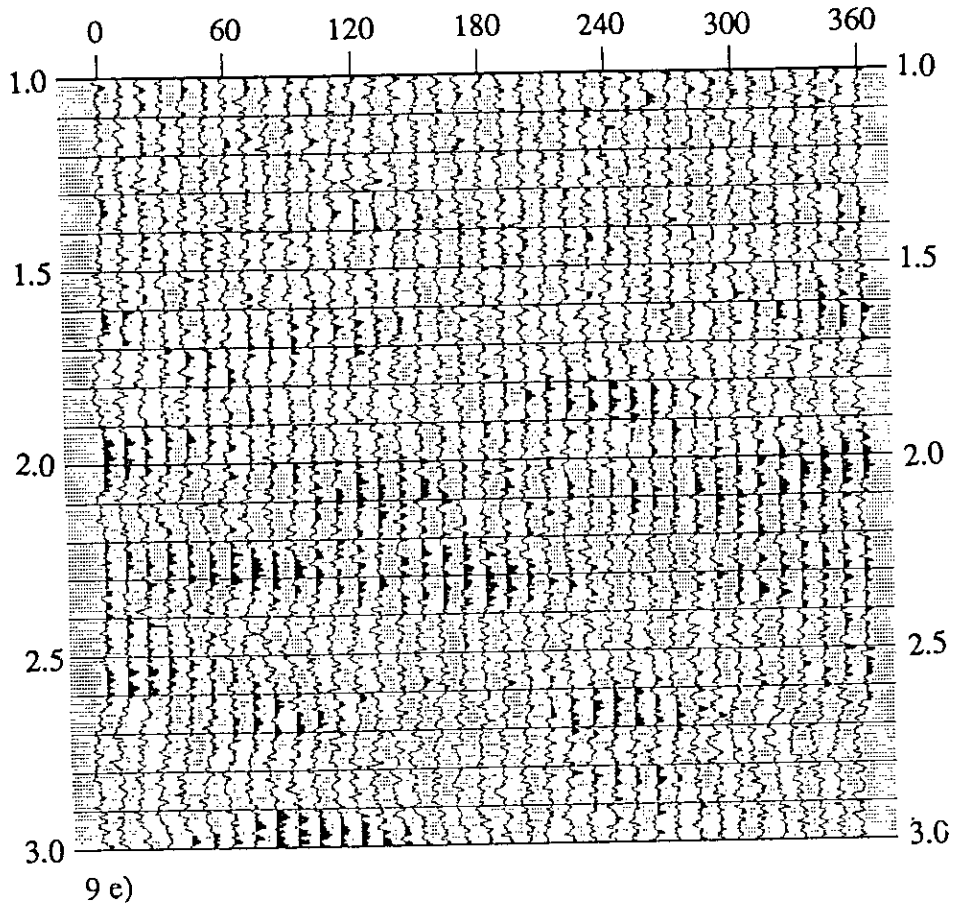

Figure 9 Shear- and compressional-wave zero-offset transmission records with different polarization from a coal sample
(a) S-wave record along short axis, direction of wave propagation is orthogonal to crack plane.
(b) P-wave record along short axis, direction of wave propagation is orthogonal to crack plane.
(c) S-wave record along short axis, direction of wave propagation is parallel to crack direction.
(d) P-wave record along short axis, direction of wave propagation is parallel to crack direction.
(e) S-wave record along long axis, direction of wave propagation is parallel to crack direction.

ACKNOWLEDGMENTS

The authors acknowledge Dr. Don C. Lawton for his constructive suggestions and Mr. Malcolm Bertram for his assistance in the *P-S* wave-separation process. Dr. Mark P. Harrison is thanked for his help in the birefringence analysis. The support of the CREWES Sponsors is much appreciated. We are especially grateful to Mobil Oil Canada for their research support and for the donation of the data.

REFERENCES

Cheadle, S.P., 1988, Applications of physical modelling and localized slant stacking to a seismic study of subsea permafrost: Ph.D.. thesis, Univ. of Calgary.

Crampin, S., 1985, Evaluation of anisotropy by shear-wave splitting: Geophysics, 50, 142-152.

DiSiena, J. P., Gaiser, J. E., and Corrigan, D., 1984, Horizontal components and shear wave analysis of three-component data, in Toksöz, M. N. and Stewart, R. R., Eds., Vertical seismic profiling, Part B: Advanced concepts: Geophysical press.

Harrison, M. P., 1992 Processing of P-SV surface-seismic data: Anisotropy analysis, dip moveout, and migration: Ph.D. Thesis, Univ. of Calgary.

Spencer, T. W., and Chi H. C., 1991, Thin-lager fracture density: Geophysics, 56, 833-843.

Stewart, R. R., 1989, VSPCCP map and AVO inversion for P-SV waves: Proc. Current. Res. Symposium, Dept. Geol. Geophys., Univ. of Calgary, 22.

Stewart, R. R., 1988, VSP imaging using converted waves: 15th Ann Nat. Mtg., Can. Soc. Expl. Geophys., Abstract, 29.

Sun, Z., Brown, R. J., Lawton, D. C., and Wang, Z., 1991, Seismic anisotropy and salt detection: A physical modelling study: 61st Ann. Internat. Mtg., Soc. Expl. Geophys., Expanded Abstracts, 713-716.

Winterstein, D., 1992, How shear-wave properties relate to rock fractures: Simple cases: The Leading Edge, 11, No. 9, 21-28